A case study on dynamic thermal imaging evaluation of a thyroid nodule

R. Vardasca[1,2,4,] C. Magalhaes[1,2], C. Freitas[3], J. Mendes[1,2]

[1]Faculdade de Engenharia, Universidade do Porto, Porto, Portugal
[2]LABIOMEP, INEGI, Porto, Portugal
[3]Endocrinology department, Centro Universitário e Hospitalar do Porto, Porto, Portugal
[4]Faculty of Computing, Engineering and Science, University of South Wales, Pontypridd, United Kingdom

SUMMARY

BACKGROUND:The thyroid gland is a butterfly-shaped organ located in the neck anteriorly to the larynx and trachea, typically extending from the level of C5-T1. It is responsible for the release of hormones that control metabolic rates and thereby modifying obligatory and adaptive thermogenesis. This organ can be affected by nodules and cellular malformations, which can result in malignant neoplasia or benign cysts. Those manifestations may change the normal pattern of skin temperature distribution in the affected area. The aim of this study is to investigate the thermal pattern of a subject presenting a hypervascularized nodule located on the left side of the thyroid.

MATERIALS AND METHODS: A male with 40 years old presenting a 11x6 mm nodule in the left side of his thyroid, confirmed by functional doppler imaging, was examined in a controlled environment using a FLIR E60 thermal camera and two aluminium disks to provide a cooling provocation during one minute on the skin, above the thyroid gland location. Thermal images were taken before and until the fifth minute after cooling at an interval of 1 minute. A 26x26 pixel square region of interest (ROI) was drawn in the analysis software to statistically analyze the temperature values, histogram, mean, median and mode temperature, standard deviation, kurtosis and skewness per ROI and side.

RESULTS:The ROI presented at baseline a bilateral difference in mean temperature of 0.4 ºC, after cooling this difference was accentuated, the affected side recovered quickly and showed a hot spot in the area of the nodule identified by Doppler imaging.

CONCLUSION:This case study showed evidence of the utility on using dynamic infrared thermal imaging when assessing thyroid nodules, which was confirmed by Doppler imaging to be highly vascularized. However, for diagnostic purposes the traditional expensive methods such as biopsy and nuclear medicine are still required. Still the application of IRT imaging should be further researched in possible monitoring and documenting the diagnosis and treatment evaluation applied to thyroid conditions.

KEY WORDS: Dynamic thermography; skin temperature; thermal symmetry; thyroid nodule

EINE FALLSTUDIE ZUR AUSWERTUNG EINES DYNAMISCHEN WÄRMEBILDES EINES SCHILDDRÜSENKNOTENS

HINTERGRUND: Die Schilddrüse ist ein schmetterlingsförmiges Organ, das sich am Hals vor dem Kehlkopf und der Luftröhre befindet und sich typischerweise auf Höhe C5-T1 erstreckt. Es ist für die Freisetzung von Hormonen verantwortlich, die Stoffwechselraten steuern und damit die obligatorische und adaptive Thermogenese verändern. Dieses Organ kann durch Knötchen und zelluläre Fehlbildungen verändert werden, die zu bösartiger Neoplasie oder gutartigen Zysten führen können. Diese Manifestationen können das normale Muster der Hauttemperaturverteilung im betroffenen Bereich verändern. Ziel dieser Studie ist es, das thermische Muster einer Person zu untersuchen, die ein hyper-vaskularisiertes Knötchen auf der linken Seite der Schilddrüse aufweist.

METHODE: Ein durch funktionelle Doppler-Bildgebung bestätigter 11x6-mm großen Knoten an der linken Seite der Schilddrüse eines 40 Jahre alten Mannes, , wurde in einer kontrollierten Umgebung mit einer FLIR E60-Wärmebildkamera untersucht, nachdem mit zwei Aluminiumscheiben die Haut über der Schilddrüsen 1 Minute lang gekühlt worden war. Wärmebilder wurden vor und bis zur fünften Minute nach der Kühlung im Minutenabstand aufgenommen. Mit der Analysesoftware wurde ein quadratischer 26x26 Pixel großer Auswertebereich (ROI) gezeichnet, um Temperaturwerte, Histogramm, Mittelwert, Median- und Modus-Wert der Temperatur, Standardabweichung, Kurtose und Schiefe pro ROI und Seite statistisch zu analysieren.

ERGEBNISSE: Zu Beginn fand sich ein Seitenunterschied der mittleren Temperatur von 0,4°C. Dieser Unterschied verstärkte nach der Kühlung, die betroffene Seite erholte sich rasch und zeigte einen Hot Spot in dem Bereich, der durch Doppler-Bildgebung als Knötchen identifiziert worden war.

SCHLUSSFOLGERUNG: Diese Fallstudie liefert Hinweise für den Nutzen der dynamischen Infrarot-Thermographie bei der Beurteilung von Schilddrüsenknoten, die durch Doppler-Bildgebung als hoch vaskularisiert bestätigt wurde. Trotzdem sind für diagnostische Zwecke die traditionellen kostspieligen Methoden wie Biopsie und Nuklearmedizin weiterhin erforderlich. Dennoch sollte die Anwendung der Infrarot-Bildgebung für eine mögliche Überwachung und Dokumentation der Diagnose und Behandlungsbewertung von Schilddrüsenerkrankungen weiter erforscht werden.

SCHLÜSELWÖRTER: Dynamische Thermographie; Hauttemperatur; thermische Symmetrie; Schilddrüsenknoten

Thermology international 2019, 29(4) 146-153

Introduction

The thyroid gland is a large endocrine gland located in the neck anteriorly to the larynx and trachea, typically extending from the level of C5- T1. Thyroid hormone influences the metabolic rate in all cells of the body and modifies many other metabolic processes in a complex interaction with other hormones. By governing the metabolism, the thyroid gland is contributing to the human homeostasis and heat production [1].

This organ can develop cellular malformations, which can result in nodules that can be benign or malignant. In case of carcinoma, it is one type of cancer that has grown in incidence over the last decade, especially in women and at an early age (2). It has a relatively low mortality rate but has a high number of recurrences (3, 4). The most common method of diagnosis is through biopsy and nuclear medicine. The common treatments available today are surgery and radiation, the surgery can be total (thyroidectomy) or partial (ablation), the radiation can be through iodine I131 or chemotherapy (5). The fact that this neoplasm is not associated with a high mortality rate lea to high treatment costs (6). The total surgery in addition to the costs of the procedure is linked to the dependency of drugs and additional costs for the lifetime (4).

Infrared thermal (IRT) imaging has already been used for designing with success a prototype of a model to aid the diagnose of thyroid gland disease (7), however advanced image processing methods and the use of dynamic thermography could improve it. The idea of using the IRT technique in the research of thyroid conditions is not new, the first suggestions were made in the 1970's (8,9), where the authors described the method as an extremely valuable new technique for the evaluation of thyroid nodules to aid the diagnosis and follow up, since it is harmless to the patients.

Other conditions that affect this gland, such as hyperthyroidism causes an increase of cutaneous temperature. Combining IRT imaging and isotope scanning was useful for investigating non-active thyroid nodules; while malignant tumors tend to present an increase in cutaneous temperature, cysts could give rise to areas of relative hypothermia. An increase in temperature was also showed in I131 active toxic adenomas (10).

Clack et al. (11) when correlating the finding of ultrasonography and IRT examination have found that there was a good correspondence between the two imaging methods but without clinical significance.

Another research (12) found no evident correlation between the thermal gradient and the clinical diameter of the thyroid nodule, the authors stated that thermography is not reliable when used to select cold thyroid nodules for surgical removal.

Helmy et al. (7) assessed the IRT potential in the detection of thyroid nodules. A cube was used as a simple geometric shape model for the neck and performed a thermal analysis based in the thyroid gland being a heat source. Finite Element Analysis was used and it was concluded that the results of the new diagnostic method were in good agreement with the current existing diagnostic method. However, this is a theoretical model and was never implemented in practice

Figure 1
Location of the thyroid gland and nodule.

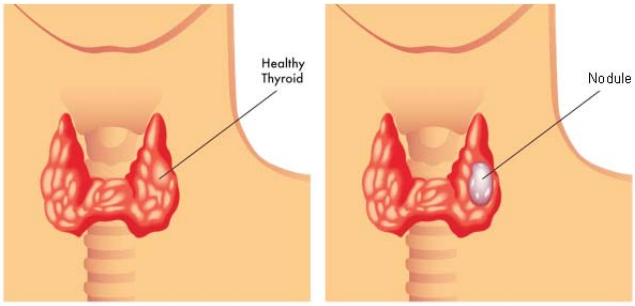

A study in Nigeria (14) concluded that IRT could be relevant, and if combined with other imaging modality could play a relevant role in the differential diagnosis of thyroid diseases, providing more complementary data in evaluation of the thyroid.

Another research using MRI and IRT imaging (14) demonstrated that thermal contributions caused by varying the breathing frequency and blood-flow velocity are negligibly small enforcing the value of using IRT in investigations of thyroid diseases.

Alves and Gabarra (15) compared the two imaging methods of IRT and power Doppler sonography in the detection of thyroid nodules, results demonstrated higher accuracy and precision of IRT in the diagnosis of thyroid nodules.

Other authors (14, 16, 17) suggest that IRT can detect thermal differences of skin overlying the thyroid, which might help to discriminate different thyroid pathological conditions.

González et al. (18) screened the neck of patients with thyroid cancer with IRT images and concluded that the method could be used as non-invasive tool for the detection of thyroid tumors. This was due to the assumed higher metabolic activity of the thyroid tumor in comparison to the healthy tissue, being the nodule detection made through the appearance of hot spots on the thermogram, which disrupts the thermal symmetry of corresponding bilateral areas.

Recent studies (19, 20) have suggested that the use of machine learning classifiers over the findings of thermal images would facilitate the diagnosis of thyroid nodules and cancer. Another research on image processing on a set of thermograms sequence (21), found that the rate of change of temperature, for every pixel within the image was of major importance. The derivation of the temperature for each pixel not only quantifies the overall rate of change of temperature associated with that pixel, but it can remove the dc offset (a non-uniformity caused by the imperfection of individual detectors and readout circuit, which is a characteristic of the technological process of recording an image) component and noise due to its intrinsic averaging func-

tion. Such algorithm would not be computationally demanding and can always guarantee convergence because only one nonlinear variable needs to be optimized, all remaining parameters being linear in nature. This processing was applied to thermal images of the neck of patients with thyroid cancer and this variation rate showed to be more adequate than mean temperatures of regions of interest.

Figure 2
The active Doppler image showing the hyper-vascularised thyroid nodule in the left lobe.

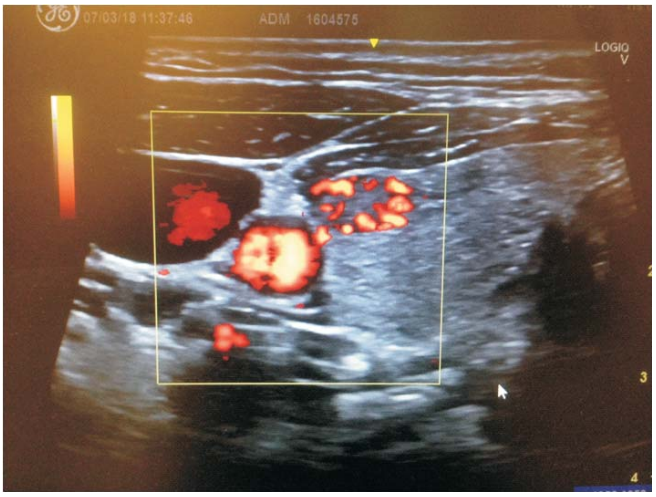

Figure 3
– The aluminum disk used for the thermal provocation over the thyroid area (diameter of 50 mm, thickness of 15 mm)

The aim of this study is to investigate the thermal pattern of a single case of a subject presenting a hypervascularized nodule located on the left side of the thyroid, through different forms of objective image analysis.

Materials and Methods

A male patient with 40 years old and a BMI of 29.7 kg/m2, was identified to have a thyroid nodule of 11x6 mm at the left side of the thyroid gland (figure 1) in an occasional Doppler scan, which also showed a hypervascularization around the nodule as presented in figure 2. The nodule was also identified by palpation.

The study took place, as suggested by IRT imaging recommendations (23-25), in an environmental controlled room of 3 x 4 m in size (with a mean temperature of 22.0 °C, relative humidity of 45%, absence of incandescent lighting over all equipment and laminar low air flow) at the Faculty of Engineering, University of Porto. For image capturing it was used a thermal camera FLIR E60 with a focal plane sensor array size of 320x240, NETD of <50 mK at 30ºC and measurement uncertainty of ±2% of the overall temperature range.

A static thermal image was taken, after the acclimatization period of 15 minutes, from the anterior view of the neck, it was followed by a contact thermal stimulus provided by

Figure 4
Analysis of the images in the FLIR ThermaCAM Researcher Pro 2.10 with the two regions of interest drawn over the thyroid gland. It is clear from the image that the left ROI presents a higher temperature than the right side.

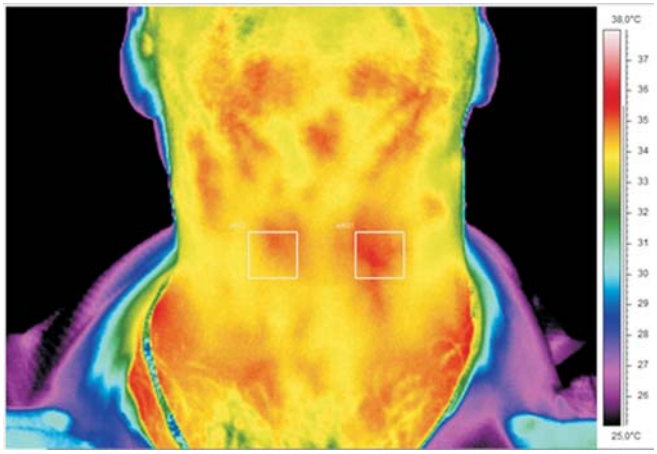

Table 1
The statistical characterization of both ROIs over the provocation test

Time	Right ROI						Left ROI					
	Mean	Median	Mode	sd	Kurtosis	Skewness	Mean	Median	Mode	sd	Kurtosis	Skewness
Baseline	34.5	34.5	34.8	0.3	- 1.23	0.01	34.9	35.0	35.1	0.2	- 0.65	- 0.13
0 min	26.4	26.4	26.4	0.1	- 0.36	0.35	26.8	26.7	26.4	0.4	0.82	0.14
1 min	29.7	29.7	29.7	0.3	0.82	0.38	30.8	30.7	30.1	0.7	- 0.2	0.71
2 min	31.0	31.0	30.9	0.3	- 0.4	0.5	32.3	32.2	32.2	0.2	- 0.48	0.49
3 min	31.7	31.7	31.6	0.3	- 0.32	0.6	32.9	32.8	32.7	0.5	- 0.59	0.31
4 min	31.8	31.7	31.5	0.4	-0.45	0.6	32.6	32.6	32.4	0.6	- 0.32	0.34
5 min	32.1	32.0	31.9	0.3	- 0.72	0.51	33.0	33.0	32.7	0.6	- 0.35	- 0.03

Figure 5
The thermal images taken during the whole dynamic test

Baseline

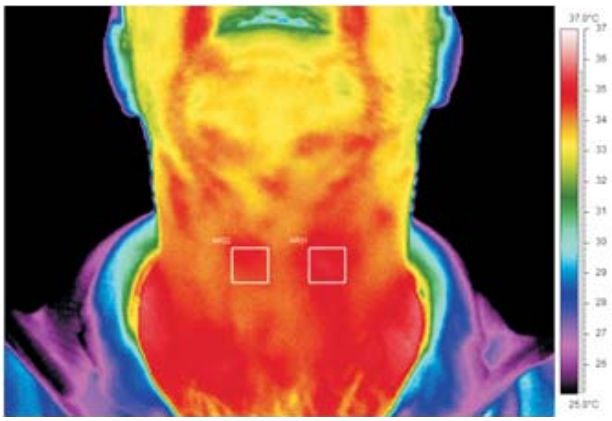

Immediately after provocation

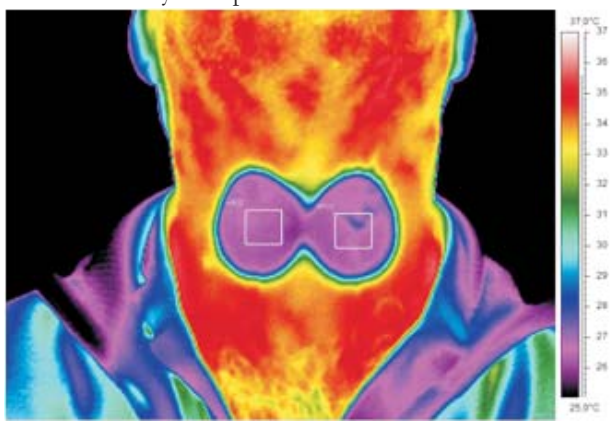

1 minute after provocation

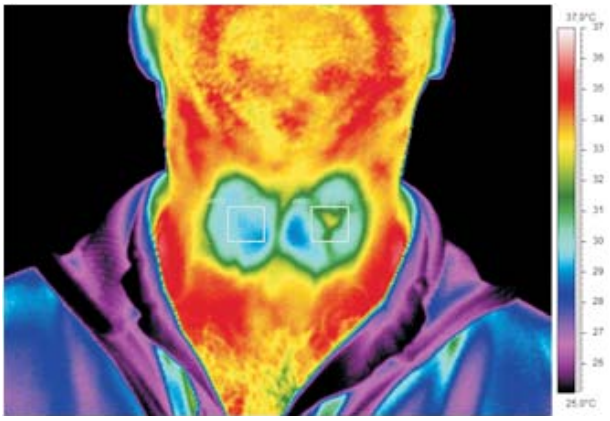

2 minutes after provocation

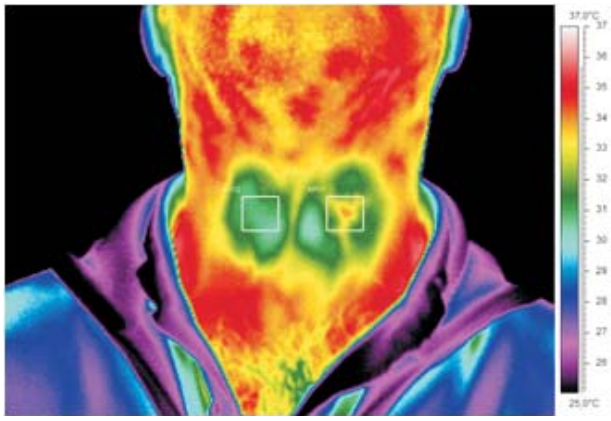

3 minutes after provocation

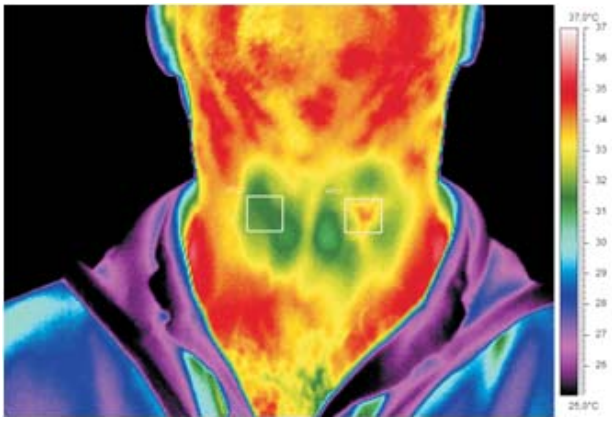

4 minutes after provocation

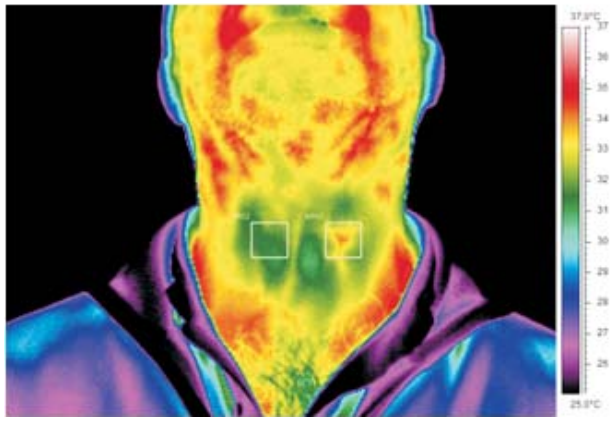

5 minutes after provocation

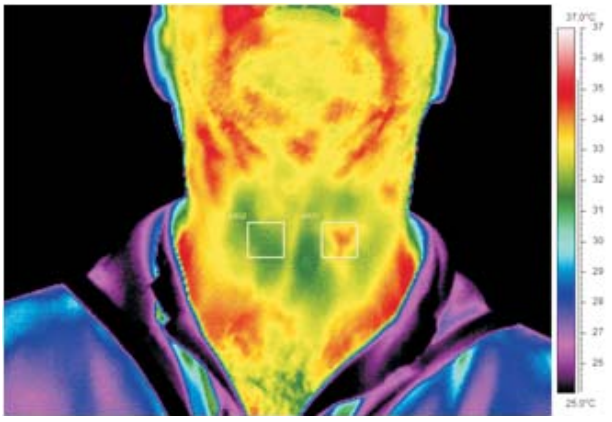

two aluminum disks with 50 mm diameter and 15 mm thick and with a surface temperature equal to examination room environmental temperature, being exposed to it during the whole acclimatization period (figure 3). The disks were applied by conduction during 1 minute on both sides of the anterior neck and above the Adam apple, 5 images were taken at 1-minute interval. Two squared regions of interest (ROI) of 26x26 pixels were drawn at the left and right side of the thyroid skin region using the software package FLIR ThermaCAM Researcher Pro 2.10 for assessing the thermal data, as presented in figure 4.

Figure 6
The histograms of the ROIs over the dynamic test.

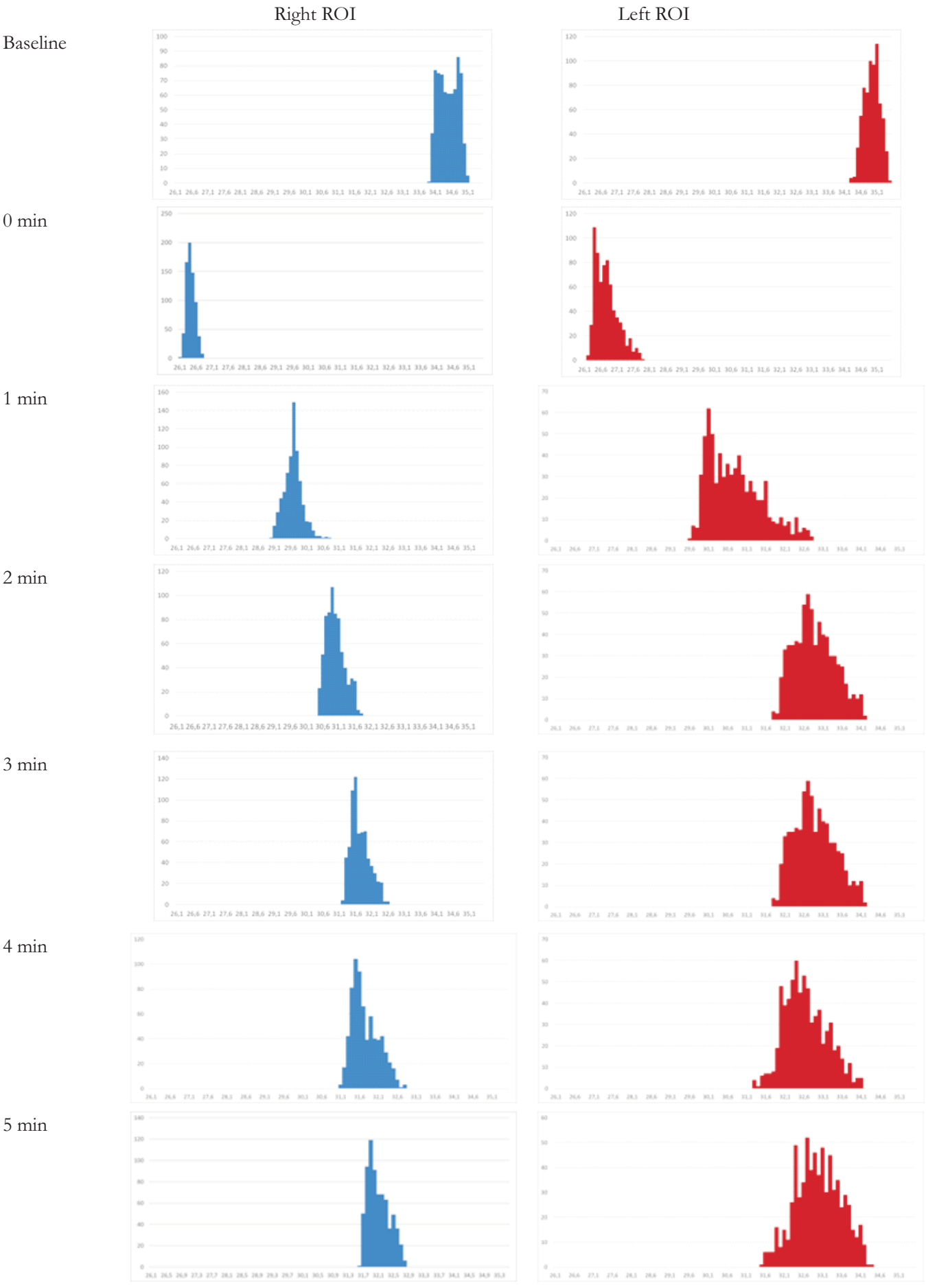

Figure 7
The characteristic charts of statistical parameter for both ROIs over the dynamic assessment.

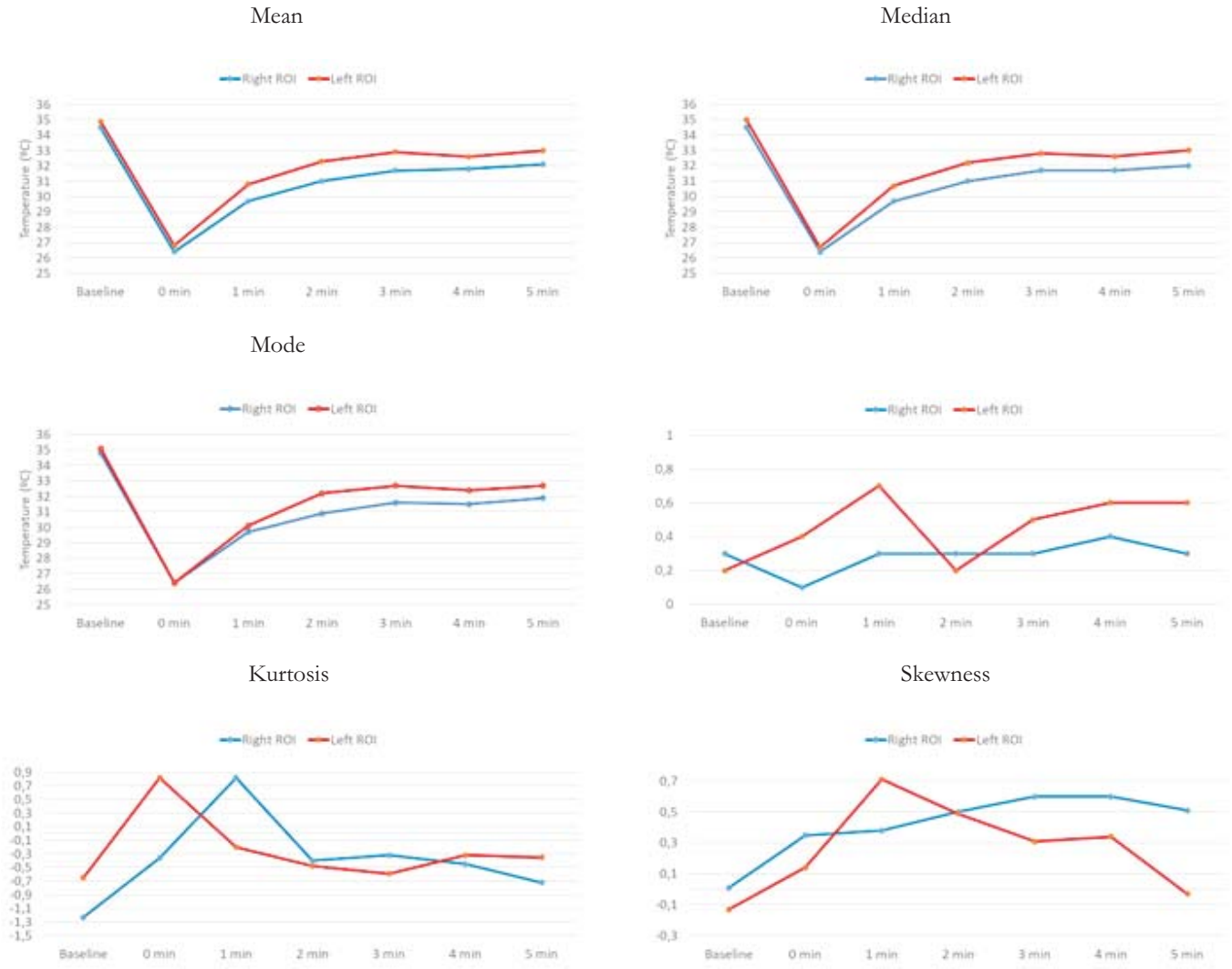

Figure 8
Thermal symmetry between bilateral ROIs along the thermal stimuli test.

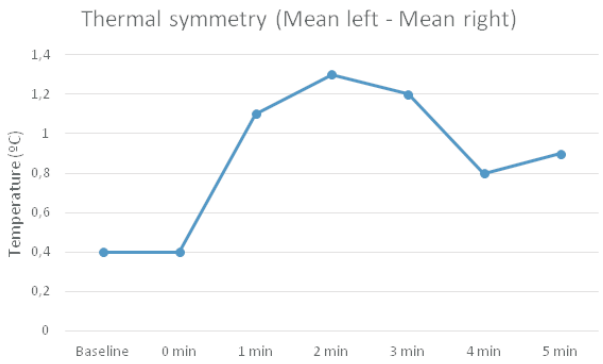

Table 2
The blood test results on the thyroid hormones values

Hormone		Normal Range
Free Thyroxin (Free T4)	1.28 ng/dL	0.93-1.7
Thyrostimulant hormone (TSH)	1.10μL/mL	0.27-4.2
Calcitonin	<2.00 pg/mL	0-20

An analysis on histogram, mean, median and mode temperature, standard deviation, kurtosis and skewness per ROI and side is performed.

Results

Table 1 presents the statistical evaluation of mean, median, mode, standard deviation, kurtosis and skewness of the 2 defined bilateral ROIs during the whole images captured within the dynamic procedure. Figure 5 shows the thermal images taken from the dynamic procedure. It can be observed that the temperature dropped after cooling with the aluminum medals and started to recover immediately after, being the recover faster at the nodule affected ROI.

Figure 6 shows the evolution of the histograms over the 6 images taken during the examination, where it can be seenat none of the histograms followed the normal distribution.

Figure 7 presents the evolution for the 2 bilateral ROIs of the mean, median and mode temperature, standard deviation, kurtosis and skewness during the whole procedure. The mean, median, mode and standard deviation followed a similar pattern. The kurtosis provides a descriptor of the

shape of a probability distribution and showed a variability during the sequence of images, being higher at the nodule side. The skewness is a measure of the asymmetry of the probability distribution, also had some variability in the sequence of thermograms, being this variability different for both ROIs, the variations are subtler in non-nodule side and with an accentuated pattern at the nodule side.

The figure 8 shows the graph of the evolution of the thermal symmetry (Left ROI mean - Right ROI mean) during the sequence of IRT images, it can be observed that this value increases with the duration of the test, being higher than 0.8 ºC.

Table 2 shows the hormone values obtained from the blood tests of the subject, which are normal.

Discussion

This study has followed the IRT imaging guidelines (22-24) with respect to examination room and equipment preparation, the hypervascularized nodule was clear in the thermograms and more evident after cooling. The correlation of the findings in both imaging modalities is in line with the existing literature (11, 15). The mean, median, mode and thermal symmetry values are useful to discriminate the affected side from the contralateral normal side. The utility of the histograms and the value of skewness is debatable in discriminating the sites. No utility was found for the kurtosis value.

The use of histograms eases the task of identifying different data, the frequency of the data occurring in the ROI dataset and categories which are difficult to interpret in a tabular form, helping to visualize the distribution of the data within that ROI. This can be of extreme importance, as shown in this example (table 3), for understanding the thermal dynamic change of the data in small ROI.

All the numeric values obtained from the sequence of images along with rate of the change in temperature per pixels inside the ROI as suggested by the literature (21) in a large database of thyroid condition patients, may be used as inputs for machine learning classifiers (19, 20), which can be an important aid for physicians in their diagnosis of thyroid diseases.

The patient of this case study has to be regularly under surveillance due to the hypervascularization of the nodule found, despite the result of the blood tests for the thyroid hormones.

Conclusion

This case study showed evidence of the utility on using dynamic infrared thermal imaging when assessing thyroid nodules, which was confirmed by Doppler imaging to be highly vascularized and presenting a higher skin temperature when compared with the contralateral side. However, for diagnostic purposes, the traditional expensive methods such as biopsy and nuclear medicine are still required.

The application of IRT imaging should be further researched in monitoring and documenting the diagnosis and treatments evaluation applied to thyroid conditions such as cancer, hypothyroidism and hyperthyroidism. The application of image processing techniques along with the statistical evaluations of ROIs should be used to populate large databases and be inputs for decision support systems using artificial intelligence methods to aid physicians in their diagnosis.

Acknowledgements

Authors acknowledge the funding of projects LAETA - UID/EMS/50022/2013.

Conflict of Interest

The authors have no conflict of interest.

References

1. Guyton AC, Hall JE. Textbook of medical physiology. 11th ed. Pennsylvania: Elsevier Saunders, 2006.

2. Garcia M, Jemal A, Ward EM, Center MM, Hao Y, Siegel RL, Thun MJ. Global Cancer Facts & Figures 2008. Atlanta, GA: American Cancer Society, 2008.

3. Brown AP, Chen J, Hitchcock YJ, Szabo A, Schrieve DC, Tward JD. The risk of second primary malignancies up to three decades after the treatment of differentiated thyroid cancer. J Clin Endocrinol Metab, 2008, 93: 504-515.

4. Brown RL, de Souza JA, Cohen EE. Thyroid cancer: burden of illness and management of disease. J. Cancer, 2011, 2: 193-199.

5. Blankenship DR, Chin E, Terris DJ. Contemporary management of thyroid cancer. Am J Otolaryngol, 2005, 26: 249 -260

6. Manikantan K, Khode S, Dwivedi RC, Palav R, Nutting CM, Rhys-Evans P, Harrington KJ, Kazi R. Making sense of post-treatment surveillance in head and neck cancer: when and what of follow-up, Cancer Treatment Reviews, 2009, 35(8): 744-753.

7. Helmy A, Holdmann M, Rizkalla M. Application of Thermography for Non-Invasive Diagnosis of Thyroid Gland Disease. IEEE Trans. Biomed. Eng., 2008, 55: 1168-1175.

8. Karpman HA. Thermography in diagnosis of thyroid nodule. JAMA, 1971, 216(10): 1646-1647.

9. Samuels BI. Thermography: a valuable tool in the detection of thyroid disease. Radiology, 1972, 102(1): 59-62.

10. Galli G, Salvo D, Troncone L, De Rossi G. Combined thermography and isotope scanning in thyroid pathology. Acta Radiologica. Diagnosis, 1974, 15(6): 656-661.

11. Clark OH, Greenspan FS, Coggs GC, Goldman L. Evaluation of solitary cold thyroid nodules by echography and thermography. The American Journal of Surgery, 1975, 130(2): 206-211.

12. Di SP, Piva LUIGI, Viganotti G, Bertario LUCIO. Critical evaluation of the use of thermography in the investigation of scintigraphically cold thyroid nodules. Investigative radiology, 1982, 17(6): 607-609.

13. Aweda MA, Adeyomoye AO, Abe GA. Thermographic analysis of thyroid diseases at the Lagos university teaching hospital, Nigeria. Adv. Appl. Sci. Res, 2012, 3: 2027-2032.

14. Jin C, He ZZ, Yang Y, Liu J. MRI-based three-dimensional thermal physiological characterization of thyroid gland of human body. Medical engineering & physics, 2014, 36(1): 16-25.

15. Alves MLD, Gabarra MHC. Comparison of power Doppler and thermography for the selection of thyroid nodules in which fine-needle aspiration biopsy is indicated. Radiol Bras., 2016, 49(5): 311-315.

16. Jiang, L. J. et al. A perspective on medical infrared imaging. Journal of medical engineering & technology, 2005, 29(6): 257-267

17. Rossato M, Burei M, Vettor R. Neck thermography in the differentiation between diffuse toxic goiter during methimazole treatment and normal thyroid. Endocrine, 2015, 48(3): 1016-1017.

18. González JR, Rodrigues EO, Damião CP, Fontes CAP, Silva AC, Paiva AC, Li H, Du C, Conci A. An Approach for Thyroid Nodule Analysis Using Thermographic Images. Application of Infrared to Biomedical Sciences, 2017: 451-475.

19. González, JR, Damião C, Conci, A. An infrared thermal images database and a new technique for thyroid nodules analysis. In MEDINFO 2017: Precision Healthcare Through Informatics: Proceedings of the 16th World Congress on Medical and Health Informatics, IOS Press, 2018, 245: 384.

20. Bahramian F, Mojra A. Analysis of thyroid thermographic images for detection of thyroid tumor: An experimental?numerical study. Int J Numer Meth Biomed Eng, 2019: e3192.

21. Chan FHY, So ATP, Kung AWC, Lam FK, Yip HCL. Thyroid diagnosis by thermogram sequence analysis. Bio-medical materials and engineering, 1995, 5(3): 169-183.

22. Ring EFJ, Ammer K. Infrared thermal imaging in medicine. Physiological measurement 2012, 33(3): R33-R46.

23. Ring EFJ, Ammer K. The technique of infrared imaging in medicine, Thermology international 2000, 10(1): 7-14.

24. Ammer K. The Glamorgan Protocol for recording and evaluation of thermal images of the human body, Thermology international 2008, 18(4): 125-144.

Address for Correspondence:

Ricardo Vardasca, Ph.D., ASIS, FRPS
Faculdade de Engenharia, Universidade do Porto,
Rua Dr. Roberto Frias S/N, 4200-465 Porto, Portugal

Email: ricardo.vardasca@fe.up.pt

(Received 07.10.2019, revision accepted 28.10.2019)